

# Design of a Continuously Controlled Linear Static Var Compensator for Load Balancing and Power Factor Correction Purposes

Abdulkareem Mokif Obais, Jagadeesh Pasupuleti

**Abstract** – In this paper a new configuration of static Var compensator is presented. The configuration is a parallel combination of a binary thyristor switched-capacitor bank (BTSCB), a binary thyristor switched-reactor bank (BTSRB), and a thyristor controlled reactor (TCR). This compensator is capable of responding equally to both capacitive and inductive reactive current or reactive power demands for load balancing and power factor correction purposes. The harmonic contents of this configuration are almost ineffective, since the TCR which is the main source of them is only representing one seventh the compensator rating. Even though the BTSCB and BTSRB are offering stepping responses, the overall compensator response is linear since the TCR functions as a linearizer between adjacent steps in both capacitive and inductive modes of operation. This compensator is characterized by the possibility of operation at higher voltage and current ratings, low no load operating losses, and no need to harmonic filtering. A complete system was designed and tested on the computer program PSpice. Copyright © 2011 Praise Worthy Prize S.r.l. - All rights reserved.

**Keywords:** Load Balancing, Power Factor, Reactive Power Control, Static Var, Voltage Control

	<b>Nomenclature</b>		
BTSCB	Binary thyristor switched-capacitor bank	$(D5^*, D6^*, D7^*)$	Most significant digits of the second analogue to digital converter
BTSRB	Binary thyristor switched-reactor bank	$V_1$	Analogue output voltage of the excessive capacitive current estimation circuit
TCR	Thyristor controlled reactor	$V_2$	Analogue output voltage of the deficient inductive current estimation circuit
$V$	a c line to line voltage	$V_3$	Toggling circuit analogue output voltage
$\omega$	ac voltage angular frequency	$i_T$	Compensator instantaneous total current
$C$	Capacitor bank basic capacitance	$V_m$	Line-to-line ac voltage amplitude
$L$	Reactor bank basic inductance		
FC-TCR	Fixed capacitor-thyristor controlled reactor		
$i_{TCR}$	Thyristor controlled reactor current		
$\sigma$	Thyristor controlled reactor firing angle		
$V_F$	Function circuit output voltage waveform		
ADC	Analogue to digital converter		
$V_m$	Compensator analogue input voltage		
$V_{ADC1}$	Analogue input voltage of first analogue to digital converter		
$V_{TOG}$	Toggling circuit triggering signal		
$i_{CB}$	Capacitor bank instantaneous current		
$(D5, D6, D7)$	Most significant digits of the first analogue to digital converter		
$V_{ADC2}$	Analogue input voltage of second analogue to digital converter		
$i_{LB}$	Reactor bank instantaneous current		

## I. Introduction

Load balancing is employed for achieving better quality for power systems [1]. It requires continuous control of generation and absorption of reactive power [2]. Synchronous motors or condensers offer possibilities of continuous control of balanced reactive power generation, but they are characterized by very slow responses and high operating losses, therefore static Var compensators appeared as good replacements of them [3]. They are less expensive than synchronous condensers and characterized by fast responses and less operating losses, but they are still needing smooth controlling criteria associated with optimal operating losses [3], [4]. Fixed capacitor thyristor controlled reactor (FC-TCR) compensators can continuously generate a controllable reactive power, but they exhibit

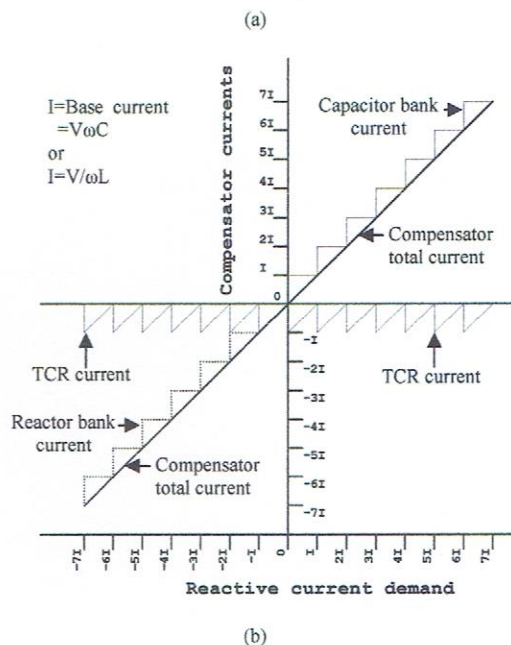
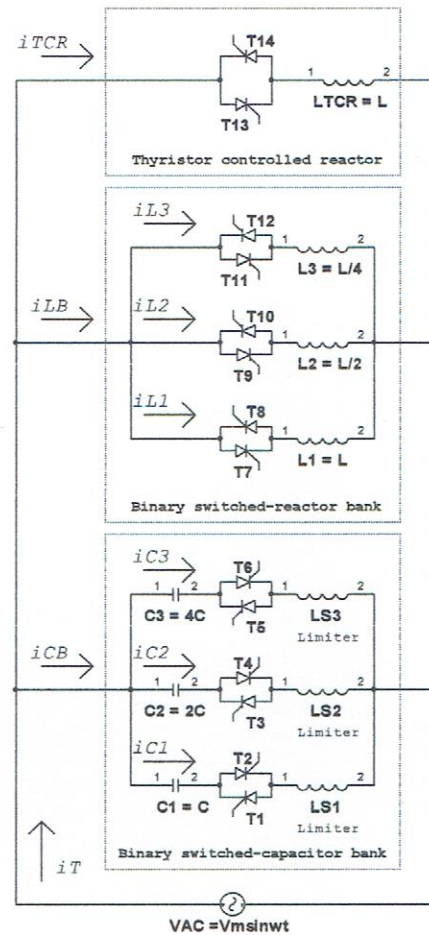
full load operating losses at no reactive power demand, since the TCR is operating at its full capacity in order to absorb the reactive power generated by the fixed capacitor [5]. The TCR is a source of harmonics, where the third harmonic for instance is about 13% of the TCR rating [4], [5]. This reveals the need for harmonics filters which add more complexity and more operating losses [6]. Switched-capacitor banks offer stepping responses in reactive power generation mode and their losses are proportional to the reactive power demands [7]. The above types of static Var compensators are called conventional types. They need medium speed solid state switching devices to function properly and hence they are less expensive [1]-[7]. A static compensator (STATCOM) which is basically built of a three phase converter shunted by a capacitor presents the feasibility of leading and lagging reactive power control [8]-[10]. This technique is restricted to low voltage applications, since it employs force-commutated fast solid-state switching devices having limited voltage and current ratings [11]. For linearity in both modes of compensation and higher voltage and current ratings purposes, an adaptive investment of conventional static Var compensators is presented in this paper for designing a new configuration responding continuously and linearly to capacitive and inductive reactive power or current demands with optimal reduction of no load operating losses and negligible harmonic contents.

## II. The Proposed Configuration

The proposed compensator is a new configuration. It is built of a binary thyristor switched-capacitor bank (BTSCB), a binary thyristor switched-reactor bank (BTSRB), and a thyristor controlled reactor (TCR). Fig. 1a shows this configuration. The BTSCB and BTSRB show stepping responses, while the TCR functions to set a linear overall response for the compensator as shown in Fig. 1(b). The TCR operates beside the BTSCB to cancel the excessive amount of capacitive reactive current and also operates with the BTSRB to compensate for the deficient inductive reactive current. The TCR rating is one seventh the BTSCB or BTSRB ratings which are  $7V\omega C$  or  $7W/\omega L$  respectively. Where  $V$  is the line-to-line voltage,  $C$  is the capacitor bank basic capacitance,  $L$  is the reactor bank basic inductance, and  $\omega$  is the power system angular frequency. This means that  $\omega C$  and  $1/\omega L$  are equal.

In this work a single limb of three identical delta-connected limbs, is considered.

At slight capacitive reactive current demand,  $C_1$  is switched on and the TCR is running at full load as stated in Fig. 1(b). This means that the no load operating losses and harmonic contents of this compensator are one seventh that of an equivalent conventional FC-TCR [4], [5]. The TCR current ( $i_{TCR}$ ) in this compensator is a source of harmonics as shown in Fig. 2.



Figs. 1. The proposed compensator, (a) configuration, (b) performance scheme

Its fundamental as a function of the firing angle  $\sigma$  is given by [4]:

$$I = \frac{V}{\pi\omega L} (\pi - 2\sigma - \sin 2\sigma) \quad (1)$$

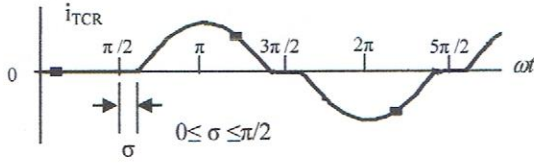


Fig. 2. The TCR current waveform

### III. Proposed System Schematic Design

A schematic diagram of the proposed system is shown in Figs. 3. The power circuit is the same as that shown in Fig. 1(a).

The timing circuit produces five voltage waveforms responsible for managing the whole compensator and guaranteeing appropriate switching for capacitors and reactors.

Fig. 3(b) shows these waveforms.  $V_F$  represents the analogue simulation of the TCR fundamental component governed by Equation (1).

This compensator is excited by the analogue voltage  $V_m$  which is directly proportional to the reactive current demand. In this work,  $V_m$  is represented by a variable voltage source. +5V and -5V refer to maximum capacitive and inductive reactive current demands respectively.

The switched-capacitor bank triggering circuit is digitally controlled by the 8-bit analogue-to-digital converter (ADC1).

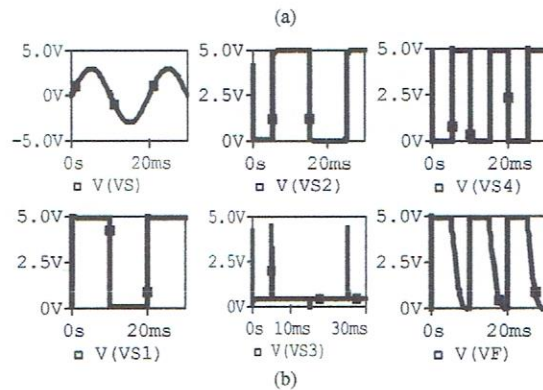
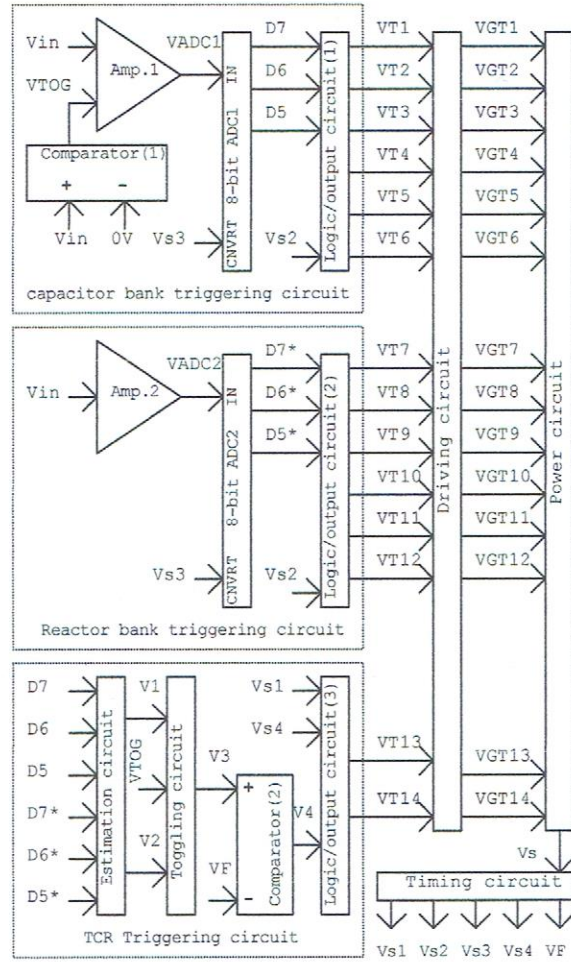
The input of ADC1 is set such that the response of this bank follows the stepping path shown in Fig. 1(b). Consequently, for values of  $V_m$  greater than zero, the analogue input of ADC1 is related to  $V_m$  as follows:

$$V_{ADC1} = \frac{14}{8} \left( V_m + \frac{V_{TOG}}{7} \right) \quad (2)$$

where  $V_{TOG}$  is +5V for  $V_m > 0$  and 0V for  $V_m \leq 0$ . The capacitor bank current ( $i_{CB}$ ) is determined by the logic status of the three most significant digits ( $D7$ ,  $D6$ , and  $D5$ ) of ADC1 as follows:

$$i_{CB} = \omega C V_m \sin \left( \omega t + \frac{\pi}{2} \right) \left[ \frac{4D7}{5} + \frac{2D6}{5} + \frac{D5}{5} \right] \quad (3)$$

where  $V_m$  is the amplitude of line-to-line voltage  $V$ . For  $D7$ ,  $D6$ , and  $D5$ , logic one corresponds to +5V and logic zero refers to 0V.



Figs. 3 The proposed compensator, (a) schematic design, (b) basic waveforms

The switched-reactor bank triggering circuit is designed such the reactor bank response follows the stepping path stated in Fig. 1(b).

Therefore the analogue input of ADC2 is related to  $V_m$  by:

$$V_{ADC2} = -\frac{14}{8}V_{in} \quad (4)$$

The reactor bank current ( $i_{LB}$ ) is given as a function of the most significant digits ( $D7^*$ ,  $D6^*$ , and  $D5^*$ ) of ADC2:

$$i_{LB} = \frac{V_m}{\omega L} \sin\left(\omega t - \frac{\pi}{2}\right) \left[ \frac{4D7^*}{5} + \frac{2D6^*}{5} + \frac{D5^*}{5} \right] \quad (5)$$

The conduction status of both capacitor and reactor banks are determined according to Table I and Table II respectively. A complete system following the schematic design steps, is implemented on the computer program PSpice as shown in Fig. 4.

Datasheets concerning all the electronic parts and aiding literatures were considered in this work [12]-[15]. The PSpice system is designed such that the capacitor bank and reactor bank are governed by the data given in Table I and Table II respectively.

In addition, the electronic circuit is designed such that the input of ADC2 is negative when  $V_m$  is greater than zero and the input of ADC1 is negative when  $V_m$  is less than zero.

This means that the capacitor bank triggering circuit will not respond during inductive reactive current demand and the reactor bank triggering circuit will not respond during capacitive reactive current demand.

TABLE I  
CAPACITOR BANK SWITCHING STATUS FOR  $0 \leq V_m \leq 5V$

$V_m$ (V)	$V_{ADC1}$ (V)	$C_1$ status	$C_2$ status	$C_3$ status
0	0	OFF	OFF	OFF
0*	1.25	ON	OFF	OFF
0.71428	2.5	OFF	ON	OFF
1.42856	3.75	ON	ON	OFF
2.14284	5	OFF	OFF	ON
2.85712	6.25	ON	OFF	ON
3.57140	7.5	OFF	ON	ON
4.28568	8.75	ON	ON	ON
5	10	ON	ON	ON

TABLE II  
REACTOR BANK SWITCHING STATUS FOR  $-5V \leq V_m \leq 0$

$V_m$ (V)	$V_{ADC2}$ (V)	$L_1$ status	$L_2$ status	$L_3$ status
0	0	OFF	OFF	OFF
-0.71428	1.25	ON	OFF	OFF
-1.42856	2.5	OFF	ON	OFF
-2.14284	3.75	ON	ON	OFF
-2.85712	5	OFF	OFF	ON
-3.57140	6.25	ON	OFF	ON
-4.28568	7.5	OFF	ON	ON
-5	8.75	ON	ON	ON

The TCR current is determined by the status of the capacitor bank and the inductor bank currents.

For the case of capacitive reactive current demand, the capacitor bank is expected to be ready for supplying the reactive current demand, but its current will rather be excessive according to its response path shown in Fig. 1(b).

The estimation circuit will produce an analogue voltage  $V_1$  proportional to that excess and is computed as follows:

$$V_1 = 7\left(\frac{4}{7}D7 + \frac{2}{7}D6 + \frac{1}{7}D5 - V_m\right) \quad (6)$$

Similarly, when the reactive current demand is inductive, the reactor bank will respond, but its current is rather insufficient to satisfy the demand. Again the estimation circuit produces an analogue voltage  $V_2$  proportional to the deficient inductive reactive current demand and is computed as follows:

$$V_2 = 7\left(-\frac{4}{7}D7^* - \frac{2}{7}D6^* - \frac{1}{7}D5^* - V_m\right) \quad (7)$$

The output of the toggling circuit  $V_3$  is toggled to  $V_1$  when  $V_m > 0$  and to  $V_2$  when  $V_m \leq 0$ . Comparator (2) determines the TCR firing angle by comparing  $V_3$  with  $V_F$  which governs the fundamental component of  $i_{TCR}$ . When  $V_3 > V_F$ , then the comparator output is logic one and is zero else where. The compensator total current  $i_T$  is given by:

$$i_T = \begin{cases} i_{CB} + i_{TCR}, & V_m > 0 \\ i_{LB} + i_{TCR}, & V_m \leq 0 \end{cases} \quad (8)$$

#### IV. Results and Discussion

The PSpice implementation of the system shown in Fig. 4 has the following basic design parameters:  $C=100\mu F$ ,  $L=99.4mH$ ,  $V_m=587V$  at a frequency of 50Hz. All performance tests were carried out at 27C°. In case of no reactive current demand ( $V_m=0$ ), no sign of significant current appears in any branch of the power circuit since the BTSCB, BTSRB, and TCR are relaxed according to the control strategy of this compensator. In case of slight capacitive reactive current demand or definitely the case at which  $V_m=0^*$  in Table I, only the capacitor  $C_1$  is expected to be switched on.

This action will stimulate the TCR to exhibit its full capacity cancelling the excess of capacitive current detected by estimation circuit. Fig. 5 shows a test demonstrating the above condition. Note that the current flowing in the capacitor  $C_1$  ( $i_{C1}$ ) and  $i_{TCR}$  cancelled each other setting a zero  $i_T$ .



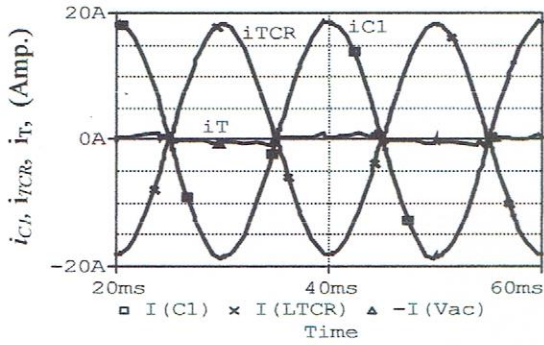
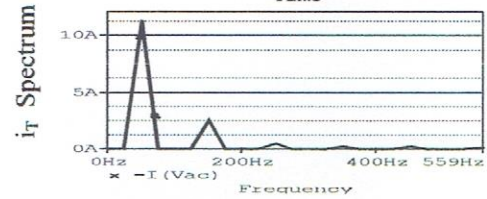
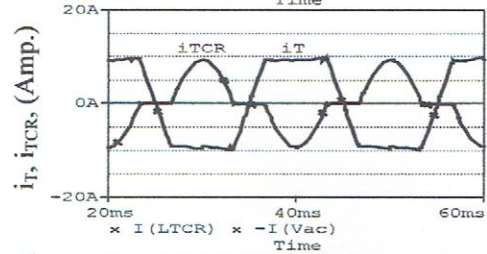
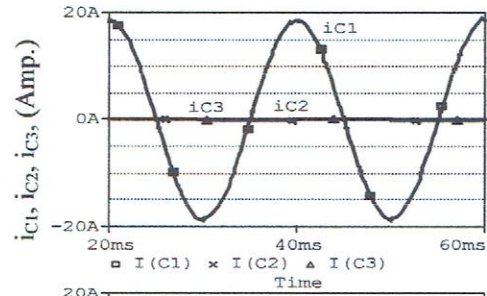


Fig. 5. Compensator status during slight capacitive current demand

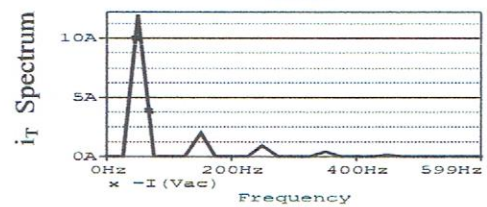
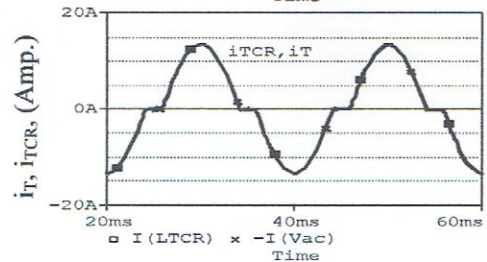
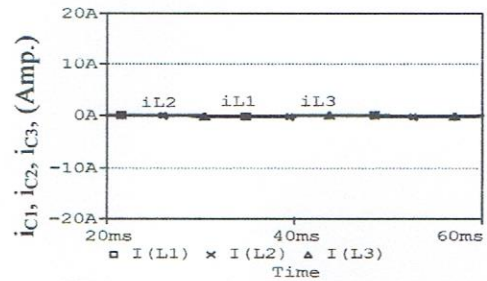
The compensator was also tested at 10% of its rating for both modes of operation. The corresponding values for  $V_m$  were +0.5V for capacitive reactive current demand and -0.5V for inductive reactive current demand. For the case of capacitive reactive demand, the capacitor  $C_1$  was switched on according to Table I supplying a reactive current of about 18.5A (peak value) which exceeded the reactive current demand by 5.6A. Consequently, the TCR was activated to absorb that excess of capacitive current as shown in Fig. 6(a). For the case of inductive current demand, only the TCR responded to that demand as shown in Fig. 6(b). Even though the compensator total current waveforms in Figs. 6 seem somewhat non-sinusoidal, their harmonic contents are almost ineffective compared to their fundamentals.

Many tests were proceeded to check compensator linearity, switching status of power circuit, and the harmonic contents at various capacitive and inductive current demands. Figures 7, 8, 9, 10 and 11 correspond to compensator performance at 20%, 40%, 60%, 80% and 100% of its rating respectively. Examining these figures, leads to a conclusion that harmonic contents are vanishing compared to compensator actual current during the increasing of reactive current demand for both modes of operation (capacitive and inductive). The dominant harmonics generated by the TCR are the third, fifth, seventh, and ninth harmonics. These harmonics were measured through many tests and no one of them touched a value of 2% of the compensator rating in both capacitive and inductive modes of operation. Theoretically, no one of harmonics in this compensator will exceed 2% of the compensator rating, since the TCR rating which is the source of them is one seventh the compensator rating.

Generally, in all tests the compensator performance follows the control strategy specified in Table I, Table II, and the estimation circuit. The overall performance of this compensator is shown in Fig. 12(a) where linearity is demonstrated within the predetermined area of operation. Fig. 12(b) shows the harmonic contents as percentages of compensator rating. Figs. 12 present this compensator as a productive tool in power quality improvement.

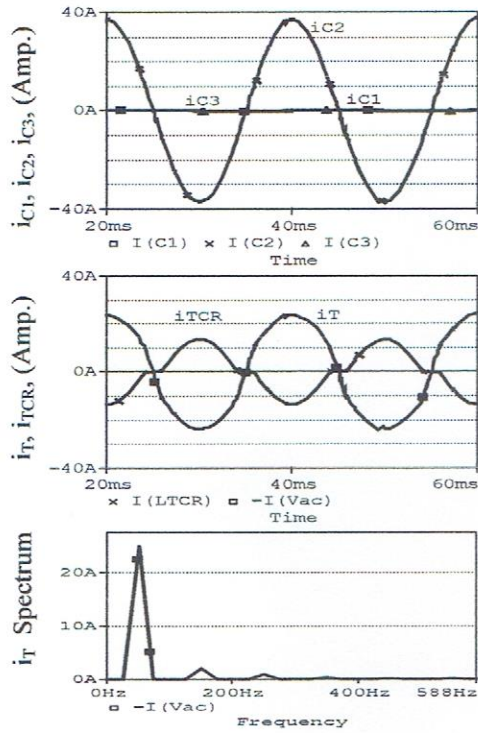


(a)

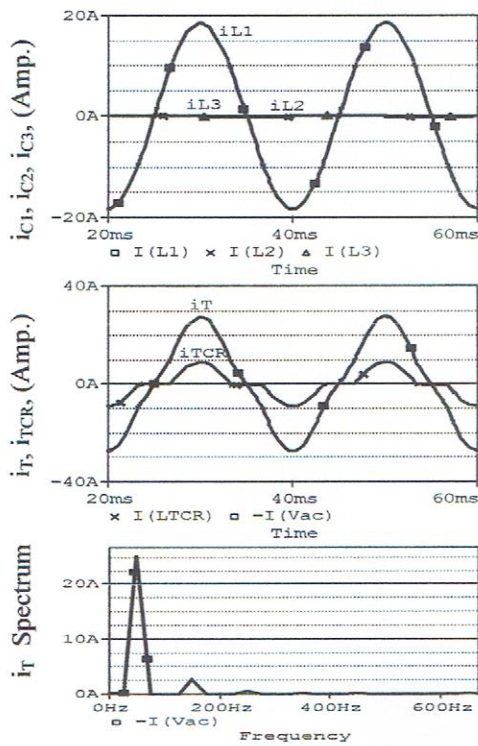


(b)

Figs. 6. Compensator response during 10% of its rating. (a) capacitive reactive current demand, (b) inductive reactive current demand

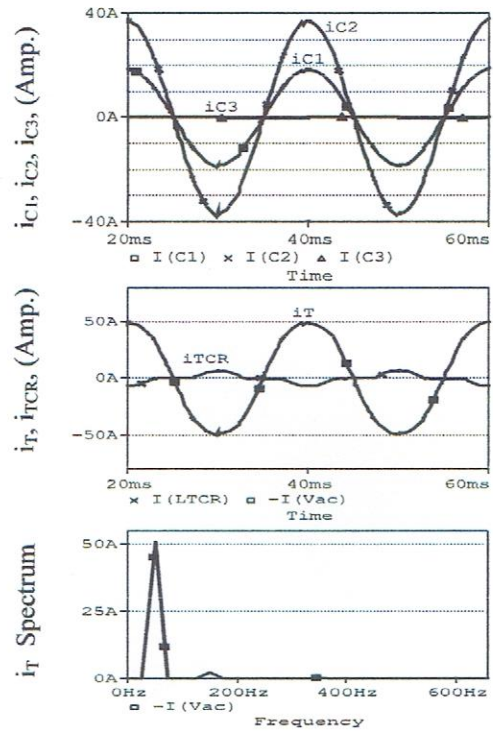


(a)

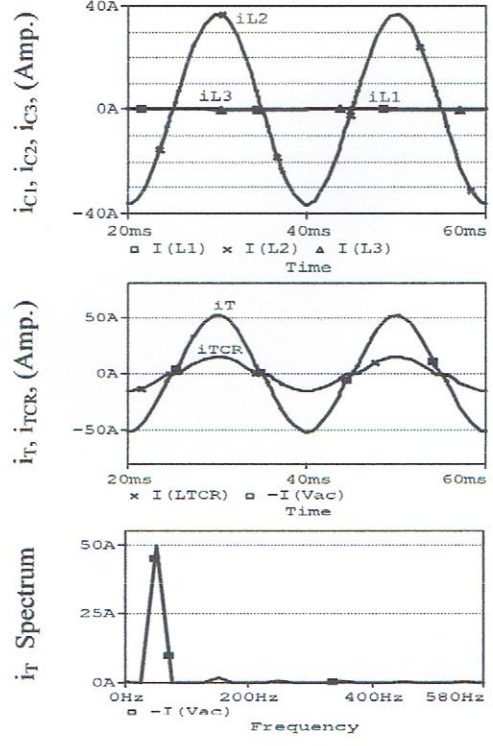


(b)

Figs. 7. Compensator response during 20% of its rating, (a) capacitive reactive current demand, (b) inductive reactive current demand

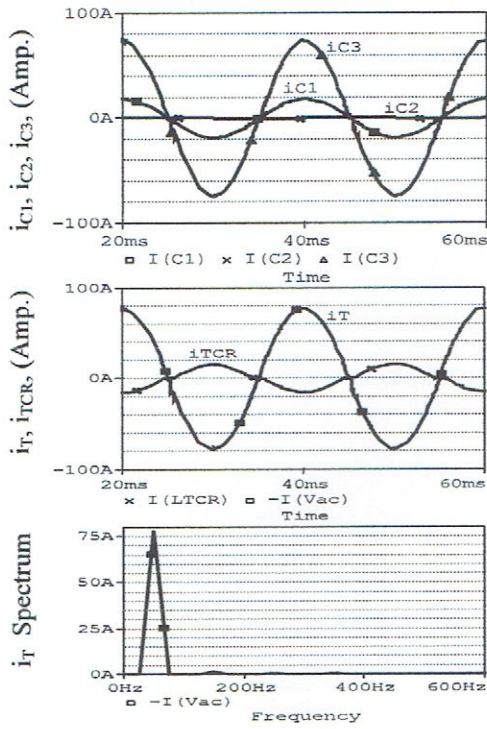


(a)

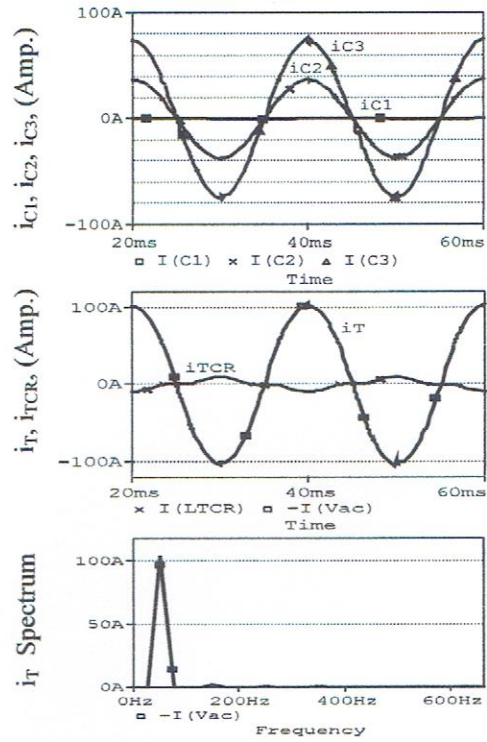


(b)

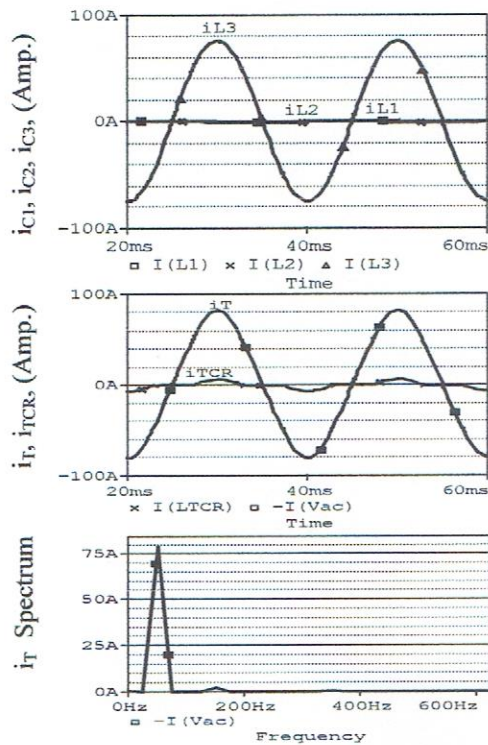
Figs. 8. Compensator response during 40% of its rating, (a) capacitive reactive current demand, (b) inductive reactive current demand



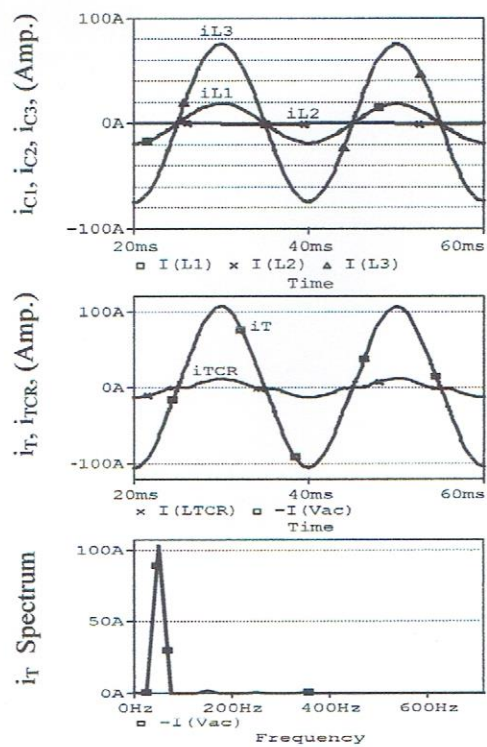
(a)



(a)



(b)

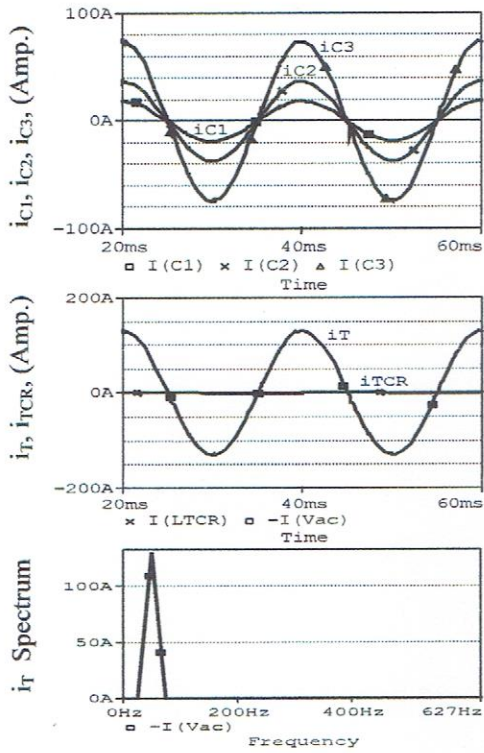


(b)

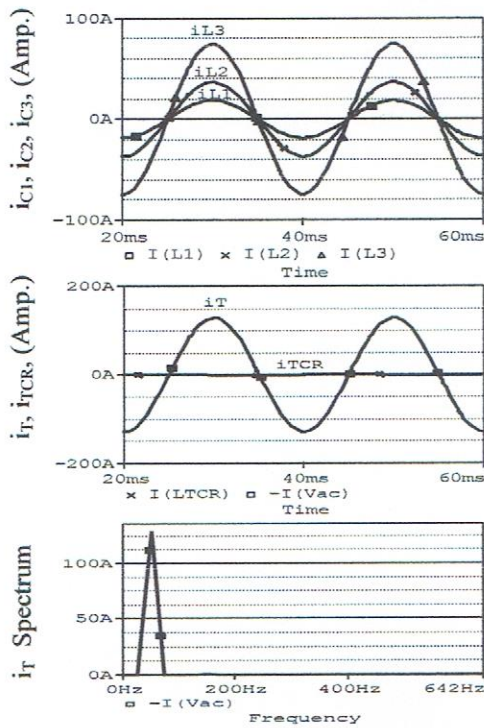
Figs. 9. Compensator response during 60% of its rating, (a) capacitive reactive current demand, (b) inductive reactive current demand

Figs. 10. Compensator response during 80% of its rating, (a) capacitive reactive current demand, (b) inductive reactive current demand



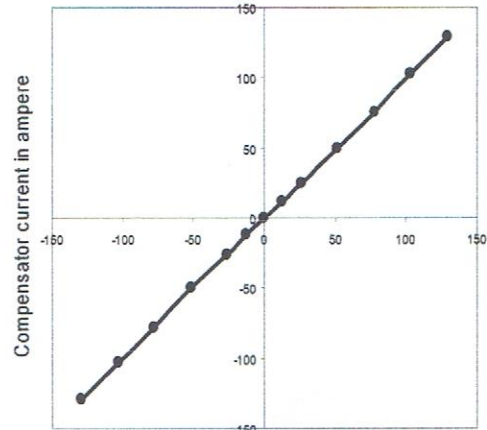


(a)

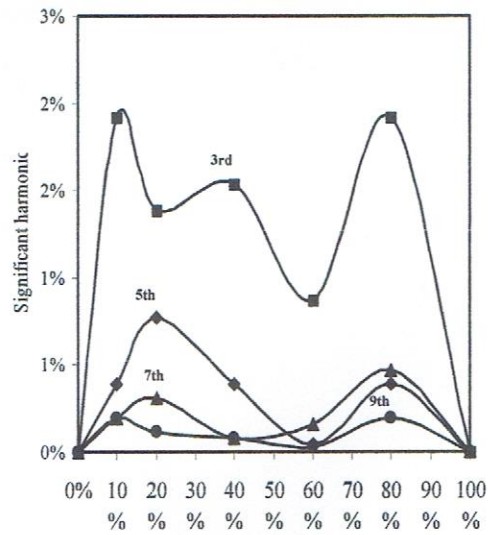


(b)

Figs. 11. Compensator response during 100% of its rating, (a) capacitive reactive current demand, (b) inductive reactive current demand



(a)



(b)

Figs. 12. Compensator overall performance, (a) linearity, (b) harmonic contents

## V. Conclusion

In this paper a single limb of a three phase compensator is designed and tested on PSpice. The three phase configuration can easily be constructed by connecting three identical limbs in delta form, installing a measuring circuit for detecting line voltages and currents, and adding a computational circuit for processing the detected voltage and current signals so as to create three controlling inputs  $V_{m1}$ ,  $V_{m2}$ , and  $V_{m3}$ . Basically, each one of these controlling signals will determine the reactive current demand for a single limb. The response of a single limb or a three phase configuration to sudden changes of reactive current demands can be settled within less than a cycle of power

system frequency, since necessary computations will be accomplished at the beginning of the second quarter of each line voltage cycle. This compensator needs no harmonic filtering; therefore it is less complicated, less dissipative, and less expensive. In addition, the compensator exhibits minimal no load operating losses compared to an equivalent FC-TCR compensator. Linearity of this compensator and feasibility of operating it at higher voltage and current ratings, assures adopting it as a competitive tool amongst load balancing techniques for achieving better power quality improvement.

## References

- [1] L. Gyugyi, Reactive Power Generation and Control by Thyristor Circuits, *IEEE Transactions on Industry Applications*, vol. IA-15 n. 5, September/October 1979, pp. 521 – 532.
- [2] L. Morán, P. D. Ziogas, G. Joos, A Solid- State High-Performance Reactive Power Compensator, *IEEE Transactions on Industry Applications*, vol. 29 n. 5, September/October 1993, pp. 969 – 978.
- [3] S. Teleke, T. Abdulahovic, T. Thiringer, J. Svensson, Dynamic Performance Comparison of Synchronous Condenser and SVC, *IEEE Transactions on Power Delivery*, vol. 23 n. 3, July 2008, pp. 1606 – 1612
- [4] R. A. Best, H. Z. La Parra, Transient Response of a Static Var Shunt Compensator, *IEEE Transactions on Power Electronics*, vol. 11 n. 3, May 1996, pp. 489 – 494.
- [5] J. H. Chen, W. J. Lee, M. S. Chen, Using a Static Var Compensator to Balance a Distribution System, *IEEE Transactions on Industry Applications*, vol. 35 n. 2, March/ April 1999, pp. 298 – 304.
- [6] S. Y. Lee, C. J. Wu, Reactive Power Compensation and Load Balancing for Unbalanced Three-Phase Four Wire System by a Combined System of an SVC and a Series Active Filter, *IEE Proc.,-Electr. Power Appl.*, Vol. 147 n. 6, November 2000, pp. 563 – 571.
- [7] S. Nandi, P. Biswas, V. N. Nandakumar, R. K. Hegde, Two Novel Schemes Suitable for Static Switching of Three-Phase Delta-Connected Capacitor Banks with Minimum Surge Current, *IEEE Transactions on Industry Applications*, vol. 33 n. 5, September/October 1997, pp. 1348 – 1354.
- [8] G. E. Valderrama, P. Mattavelli, A. M. Stanković, Reactive Power and Unbalance Compensation Using STATCOM with Dissipativity-Based Control, *IEEE Transactions on Control Systems Technology*, vol. 9 n. 5, September 2001, pp. 718 – 727.
- [9] R. Mohamad Idris, A. Khairuddin, M. W. Mustafa, A. Kalam, Optimal Allocation of Multi-Type FACTS Devices Using Bees Algorithm for ATC Enhancement in Deregulated Power System, *International Review on Electrical Engineering (IREE)*, vol. 5 n. 2, March/ April 2010, pp. 644 – 651.
- [10] Mehdi Safaeian, Mehdi Abapoor, Power Compensation and Power Factor Correction Using Fuzzy Logic Based SVC, *International Review on Modelling and Simulations (IREMOS)*, vol. 3 n. 6, December 2010, pp. 1382 – 1387.
- [11] Y. Xu, L. M. Tolbert, J. D. Kueck, D. T. Rizy, Voltage and Current Unbalance Compensation Using a Static Var Compensator, *IET Power Electron.*, Vol. 3 Iss. 6, August 2010, pp. 977 – 988.
- [12] H. Malmstadt., C. Enke, S. Crouch, *Electronics and Instrumentation for Scientists* (The Benjamin/ Cumming Company, Inc., 1981).
- [13] M. Rashid, *Power Electronics Handbook* (Academic Press, 2001).
- [14] T. Skvarenina, *The Power Electronics Handbook* (Marcel CRC Press, 2002).
- [15] K. B. Bimal, *Power Electronics and Motor Drives* (Elsevier Inc., 2006).

## Acknowledgements

This work was accomplished in Universiti Tenaga Nasional, Malaysia.

## Authors' information



**Abdulkareem Mokif Obais** received B.Sc. degree in Electrical Engineering from Baghdad University, Iraq, in 1982 and the M.Sc. degree in Electrical Engineering majoring in power electronics from Baghdad University, Iraq, in 1987.

He has published papers in Iraqi Journals in the fields of power electronics and participated in many annual scientific conferences in Iraq. His research interests are in induction heating, load balancing, reactive power control, static Var compensators, STATCOMs, ac and dc drives. He is a Professor in Electrical Engineering Department / College of Engineering / University of Babylon in Iraq. Presently, he is preparing for his PhD degree in Universiti Tenaga Nasional, Malaysia.



**Dr. Jagadeesh Pasupuleti** was born in Vadamalapeta, India. He has received B.Tech degree in Electrical & Electronics Engineering from Nagarjuna University, India, in 1986 and, the M.Tech and Ph.D. degrees in Electrical & Electronics Engineering majoring in power system operation & control from Sri Venkateswara University, India, in 1988 and

2002 respectively.

He has published papers in International Conference Proceedings and International Journals in the fields of power system operation & control and renewable energy. His research interests are in power system operation & control, application of power electronics and renewable energy.

Dr.Pasupuleti is a Senior Member of IEEE, Member of IET and ISTE and C.Eng. of EC UK.